Evidence for superior current carrying capability of iron pnictide tapes under hydrostatic pressure

Babar Shabbir,[1] He Huang,[2] Chao Yao,[2] Yanwei Ma,[2,*] Shixue Dou,[1] Tom H. Johansen,[1,3]
Hideo Hosono,[4] and Xiaolin Wang[1,†]

[1]*Institute for Superconducting and Electronic Materials, Australian Institute for Innovative Materials, University of Wollongong, North Wollongong, New South Wales 2522, Australia*

[2]*Key Laboratory of Applied Superconductivity, Institute of Electrical Engineering, Chinese Academy of Sciences, 2703, Beijing 100190, China*

[3]*Department of Physics, University of Oslo, POB 1048 Blindern, 0316 Oslo, Norway*

[4]*Institute for Innovative Research, Materials and Structures Laboratory, Tokyo Institute of Technology, 4259 Nagatsuta, Midori-ku, Yokohama 226-8503, Japan*

(Received 2 July 2017; published 20 September 2017)

High critical current density (J_c) values in superconducting wires/tapes are desirable for high magnetic field applications. Recently developed pnictide wires/tapes exhibit exceptional superconducting properties such as high critical temperature (T_c), upper critical field (H_{c2}), and almost field-independent J_c. Despite the great fabrication efforts, however, the newly discovered pnictide wires/tapes are still not able to replace low-temperature superconductors such as Nb_3Sn, due to their inferior J_c values. Ag-clad $Sr_{0.6}K_{0.4}Fe_2As_2$ tapes have demonstrated significant superconducting performance, although their low J_c in comparison to Nb_3Sn is still a major challenge. By successfully employing hydrostatic pressure, a remarkably significant enhancement of J_c by an order of magnitude can be achieved in $Sr_{0.6}K_{0.4}Fe_2As_2$ tapes in both low and high fields. This is a promising technological step forward towards high-field applications, as the record high J_c values ($\sim 2 \times 10^5$ A/cm^2 at 4.2 K and 13 T, $P = 1.1$ GPa) obtained for $Sr_{0.6}K_{0.4}Fe_2As_2$ tape are superior to those of Nb_3Sn and other pnictide wires/tapes. Here, we used magnetic J_c data for comparison to the other reported transport J_c data, due to the lack of transport measurement facility under hydrostatic pressure. Our systematic analysis shows that pressure-induced pinning centers are the main source of J_c enhancement, along with a fractional contribution from geometric changes around the grain boundaries under pressure. We expect that utilization of an appropriate pressure approach will be a way to significantly enhance J_c to beyond the cutoff (maximum) values in various superconductors produced using other existing methods for J_c enhancement.

DOI: 10.1103/PhysRevMaterials.1.044805

I. INTRODUCTION

Iron-based superconductors are the most technologically suitable candidates for some applications because of their high critical temperature (T_c up to 56 K), high upper critical field, $H_{c2}(0)$ (more than 100 T), low anisotropy (around 1–8), and high critical current density, J_c, values, as high as $10^6 - 10^7$A/cm^2 at low temperatures, which are essential for many applications [1–7]. Even though the high-T_c cuprate wires/tapes have achieved the highest J_c values among all the superconductors, their crystal structure, including misoriented grain boundaries, brittle texture, and extremely high anisotropy, which can increase their manufacturing costs, imposes many restrictions on their physical properties and fabrication, especially in bulk polycrystalline form [8,9]. On the other hand, the strong field dependence of the superconductivity in brittle MgB_2 limits its technological use. Thus, high-field superconducting applications are still dominated by the low T_c ($\sim$18 K) superconductor Nb_3Sn. The intermetallic Nb_3Sn can support $J_c > 10^5$ A/cm^2 up to nearly 9 T at 4.2 K. Nevertheless, Nb_3Sn tapes/wires also have the mechanical disadvantage of being very brittle and typically require a post-winding heat treatment, which is a technically challenging manufacturing step. Furthermore, its high sensitivity to strain is also problematic in high-field magnet applications, where thermal contraction differences between materials and Lorentz forces may result in a significant reduction in Nb_3Sn performance [10].

As a result, significant research and development have been undertaken to fabricate pnictide tapes/wires so that they might replace low-temperature superconductors, especially Nb_3Sn, in high-field applications. J_c values of $\sim 10^4 - 10^5$ A/cm^2 have been achieved at 4.2 K and 10 T in 122 pnictide wires/tapes by using various fabrication techniques, which include chemical additives, rolling texture, hot isostatic pressing, uniaxial hot pressing, cold pressing, and cycles of cold deformation and heat [11–13]. Ag-clad $Sr_{0.6}K_{0.4}Fe_2As_2$ tapes showed especially high J_c values ($\sim 10^5$ A/cm^2) compared with other pnictide wires/tapes, NbTi, and MgB_2 ($J_c \sim 10^4$ A/cm^2) at 4.2 K and 10 T, but their J_c was still lower than that of Nb_3Sn ($\sim 10^5$ A/cm^2 at 4.2 K and13 T) [14–16]. Achieving higher J_c values than Nb_3Sn is a new challenging aim, despite the great progress that has already been made in fabrication. While keeping in mind these limitations, *in situ* creation of new effective pinning centers can be very beneficial for further improving the current carrying capabilities in optimally doped pnictide wires/tapes. Therefore, we will show that employing hydrostatic pressure will be a useful technique to increase the number density of pinning centers and J_c values in pnictide tapes/wires.

In this paper, we investigate the effects of hydrostatic pressure on the current carrying capability of iron-based superconducting tapes for the first time in order to increase the J_c beyond certain values that have been achieved with other J_c

*Corresponding author: ywma@mail.iee.ac.cn
†Corresponding author: xiaolin@uow.edu.au

enhancement approaches. We have used optimally doped Ag-clad $Sr_{0.6}K_{0.4}Fe_2As_2$ tapes for our measurements because of their excellent recently discovered superconducting properties, and also to see whether hydrostatic pressure can raise J_c further in high-performing tapes. We found that hydrostatic pressure of 1 GPa can significantly enhance J_c in Ag-clad $Sr_{0.6}K_{0.4}Fe_2As_2$ tapes by an order of magnitude at different temperatures. This was true over an especially wide range of fields (both low and high fields), which is usually not found in other methods for the enhancement of J_c. Remarkably, our J_c values obtained under pressure ($\sim 2 \times 10^5$ A/cm^2 at 4.2 K and 13 T) in Ag-clad $Sr_{0.6}K_{0.4}Fe_2As_2$ tape are the record highest compared to other iron pnictide wires/tapes and also to Nb_3Sn, which could open up a possibilty to significantly enhance J_c to beyond the cutoff (maximum) values in various superconductors produced using other existing methods for J_c enhancement. It is important to mention here that we compared our magnetic J_c data to the other reported transport J_c data because it is not possible to measure transport J_c under the hydrostatic pressure, as this facility is not available on any transport measurement system, at present. Furthermore, we have also systematically investigated various explanations for the enhancement of J_c under pressure. We argue here that our hydrostatic pressure approach can also be very useful to further enhance J_c in other types of superconductors.

II. EXPERIMENTAL METHODS

The Ag-clad $Sr_{0.6}K_{0.4}Fe_2As_2$ tape samples with Sn addition were fabricated by the *ex situ* powder in tube (PIT) methods; the $Sr_{0.6}K_{0.4}Fe_2As_2$ powder was packed into Ag tubes with OD 8 mm and ID 5 mm. These tubes were sealed and then cold worked into tapes (about 0.4 mm in thickness) by drawing and flat rolling. For the hot pressed samples, the flat rolled monofilament tapes were sandwiched between two pieces of metal sheets and pressed with 0.25 mm in thickness. The detailed process can be found in Ref. [11]. The $M - H$ loops at different temperatures and pressures and the temperature dependence of the magnetic moments were measured on a Quantum Design physical properties measurement system (QD PPMS 14 T) by using the vibrating sample magnetometer (VSM) option. We used an HMD (manufacturer name) high-pressure cell and Daphne 7373 oil as the medium for applying hydrostatic pressure on our samples. We approximate the applied pressure by measuring the cell compression. Further details can be found in the pressure cell manual, i.e., the Quantum Design (QD) high-pressure cell user manual for use with the QD VSM, No. CC-Spr-Φ8.5D-MC4. The tape size used for measurements is $3 \times 2 \times 1$ mm^3 and the magnetic fields were applied parallel to the tape surface. In addition, the field 50 Oe is applied to measure the FC-ZFC curves.

III. RESULTS

Figure 1 shows the field-cooling (FC) and zero-field-cooling (ZFC) curves at 0, 0.25, 0.7, and 1.1 GPa. The results indicate an increase in the superconducting volume fraction and T_c (obtained from the ZFC derivative peaks, inset of Fig. 1), which improve from 29.64 K at $P = 0$ GPa to 31.12 K at $P = 1.1$ GPa at a rate of 1.43 K/GPa. The T_c, volume V,

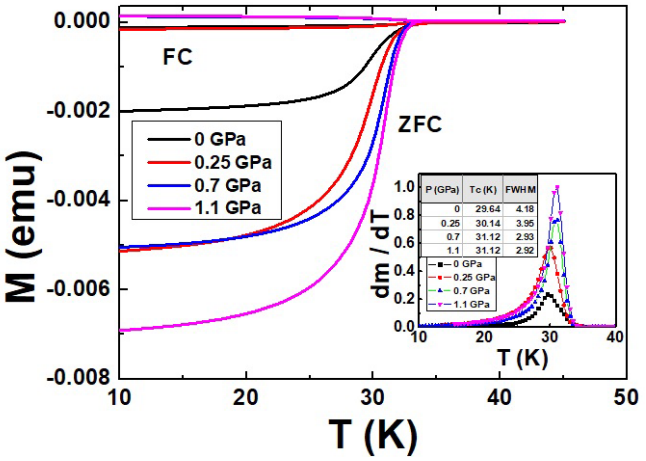

FIG. 1. Temperature dependence of the magnetic moment under applied pressure in both ZFC and FC runs. The inset shows the pressure dependence of the T_c for Ag-clad $Sr_{0.6}K_{0.4}Fe_2As_2$ tapes. T_c increases with a slope of $dT_c/dP = 1.43$ K/GPa . The inset shows ZFC derivative plots, and the inset table shows T_c along with the full width at half maximum (FWHM) values at different pressures.

and anisotropy γ of a material under pressure are interrelated as [17]

$$\Delta T_c'(P) + \Delta V' + \Delta \gamma' = 0, \tag{1}$$

where

$$\Delta T_c'(P) = \left[\frac{T_c(P) - T_c(0)}{T_c(0)}\right], \quad \Delta V' = \left[\frac{V(P) - V(0)}{V(0)}\right],$$

and $$\Delta \gamma' = \left[\frac{\gamma(P) - \gamma(0)}{\gamma(0)}\right].$$

The $\Delta V'$ at $P = 1$ GPa can be nearly estimated by

$$\Delta V' = -\Delta P/B, \tag{2}$$

where B is the bulk modulus.

For bulk modulus $B \sim 62.5$ GPa (bulk modulus of a similar material, $SrFe_2As_2$), or $\Delta V' \sim -0.016$ and the experimentally obtained $\Delta T_c'(P) \sim 0.0499$, we can therefore determine that the anisotropy $\gamma(P) \approx 0.966\gamma(0)$, which shows a slight decrease in the anisotropy of $Sr_{0.6}K_{0.4}Fe_2As_2$ tape under hydrostatic pressure. The slight increase of T_c due to pressure characteristically mirrors the behavior of the anisotropy. Although a slight increase in T_c under pressure has been observed in optimally doped $Sr_{0.6}K_{0.4}Fe_2As_2$ tape, the transition width estimated from the full width at half maximum (FWHM) of the corresponding derivative peak, as plotted in the inset of Fig. 1, is actually decreased from 4.18 K at $P = 0$ GPa to 2.92 K at $P = 1.1$ GPa, which shows that the quality of the tape does not deteriorate under pressure.

We used Bean's model to estimate the field dependence of J_c at several pressures and temperatures, and the results are plotted in Fig. 2 [18]. Pressure can significantly enhance J_c at different temperatures and over a wide range of fields, which is uncommon with other J_c enhancement techniques such as high-energy ion irradiation or chemical doping. At

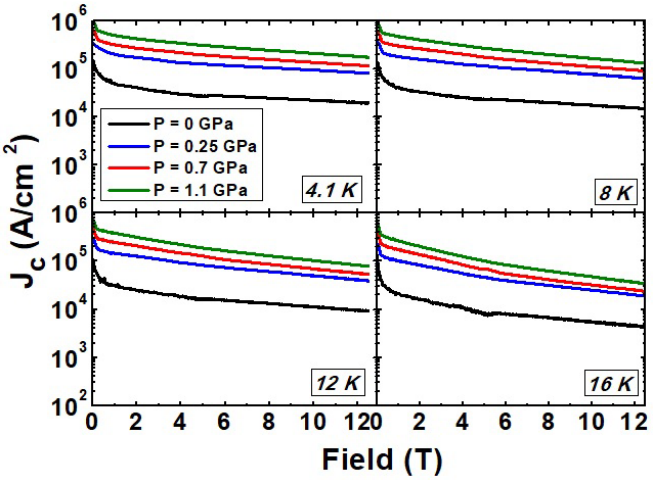

FIG. 2. Field dependence of critical current density under different pressures measured at 4.2 K, 8 K, 12 K, and 16 K. At different temperatures, J_c is enhanced under pressure by an order of magnitude and by the same amount in both low and high fields.

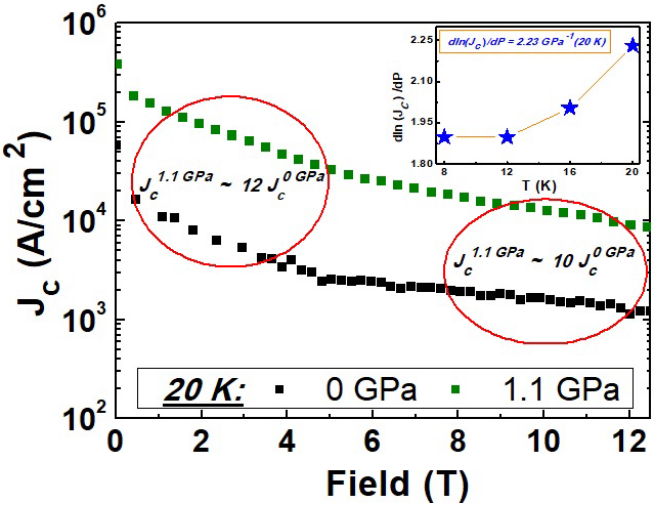

FIG. 3. Field dependence of J_c at $P = 0$ GPa and 1.1 GPa at 20 K. J_c at 1.1 GPa is enhanced by nearly 12 times in both low and high fields. The inset shows the plot of $d(\ln J_c)/dP$ versus temperature, which indicates enhancement in J_c at a rate of nearly 2.23 GPa^{-1} at 20 K in zero field.

4.2 K, the J_c values of $Sr_{0.6}K_{0.4}Fe_2As_2$ tapes approach nearly 10^6 A/cm^2 at low fields, and $\sim 2 \times 10^5$ A/cm^2 at 13 T. Even at 20 K, the J_c was increased above 10^5A/cm^2 at low fields, and 10^4A/cm^2 at high fields up to 13 T. This opens a possibility for such tapes being useful for high magnetic field applications, such as magnetic resonance imaging (MRI) machines, because they can operate in temperatures around 20 K, where cryocoolers can be used instead of liquid helium for cooling. Additionally, at 16 K and near zero field, we find a value of $J_c \sim 3 \times 10^5$ A/cm^2 under $P = 1.1$ GPa, which is higher by nearly one order of magnitude than the $J_c \sim 2 \times 10^4$ A/cm^2 under $P = 0$ GPa, with the tapes showing significant superconducting performance at a rather high temperature, in contrast to low-temperature superconductors. We also highlight another major result here as follows.

J_c enhancement by nearly an equal amount (almost tenfold for 20 K) is found in $Sr_{0.6}K_{0.4}Fe_2As_2$ tapes over a wide range of field, as demonstrated in Fig. 3, which indicates a great improvement in flux pinning. Additionally, the plot of $d(\ln J_c)/dP$ versus temperature (inset of Fig. 3) determines the J_c enhancement rate, which is found to lie between 1.85 – 2.23 GPa^{-1} (almost the same) for different temperatures at zero field, which is evidence of weak temperature dependency.

To correlate J_c, field, and pressure, we have plotted the $\ln J_c$ values versus pressure at different fixed fields and temperatures in Fig. 4. The red solid line shows linear fits to the data. Although the data points at 0.7 GPa are not properly overlapped, we have used it here for rough estimations. The slope of $\ln J_c$ versus P, $(d \ln J_c/dP)$, is nearly 1.3, 2.25, and 2 GPa^{-1} and 2, 2.25, and 2.2 GPa^{-1} at 0, 6, and 12 T for the 4 K and 8 K results, respectively. Albeit rough, the similar $d(\ln J_c)/dP$ slope values (inset) show that the J_c enhancement is nearly the same under pressure at different fields, which also demonstrates the weakly field-dependent nature of J_c for $Sr_{0.6}K_{0.4}Fe_2As_2$ tapes under pressure.

This lack of field dependence is also further reflected in Fig. 5, which compares J_c enhancement trends under pressure in pnictide tape, single crystal, and polycrystalline bulk [19,20]. It is interesting to see their diverse trends in J_c enhancement. The obtained trend is nearly steady in the tape, in contrast to the single crystal and polycrystalline bulk, where linear behavior is observed. Further analysis (Fig. 6) comparing our J_c data under pressure and J_c for conventional NbTi and Nb_3Sn superconducting wires, along with the best recently published results for pnictide wires/tapes so far, indicates that our achieved J_c values ($\sim 2 \times 10^5$ A/cm^2 at 4.2 K and 13 T) in $Sr_{0.6}K_{0.4}Fe_2As_2$ tapes under pressure are record high at 4.2 K [15,16,21–26]. The key indicator for comparison is that our J_c values are better than those of Nb_3Sn, which is an innovative result. It is also interesting to see that J_c decays

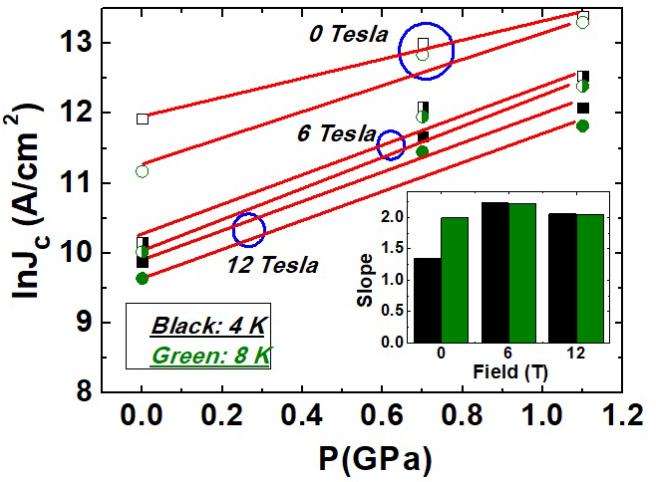

FIG. 4. Pressure dependence of J_c (logarithmic scale) at 4 K and 8 K for 0, 6, and 12 T. The solid lines are linear fits to the data, and the corresponding values of the slopes are plotted in the inset, which suggests that J_c enhancement is nearly the same in different fields, with a slightly higher value at 6 T.

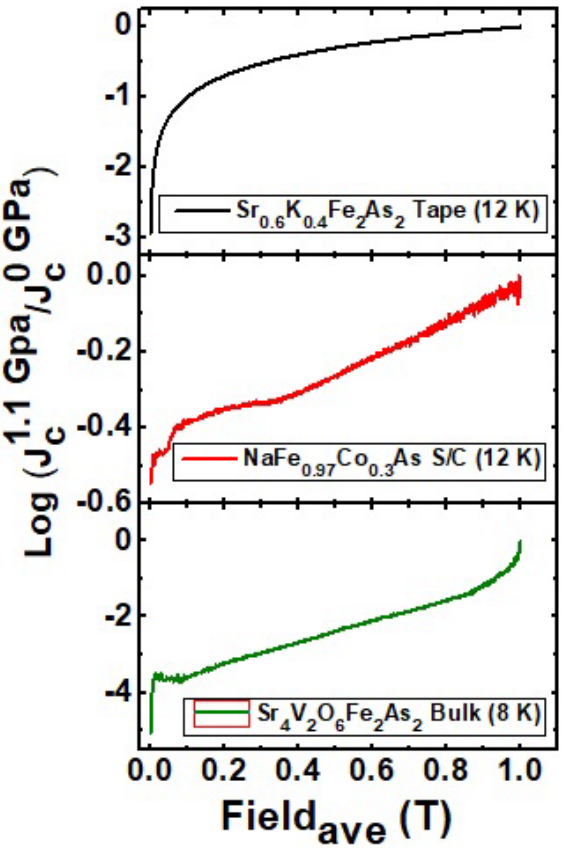

FIG. 5. Trends of J_c enhancement ratios (normalized data) for tape, single-crystal, and polycrystalline bulk samples with and without pressure versus average field. The obtained trend is nearly steady in the tape (shows weak field dependency), in contrast to the single crystal and polycrystalline bulk, where linear behavior is observed.

slowly in high fields, unlike Nb_3Sn and NbTi, which is a very desirable characteristic for high-field applications. With such weak field dependence, as is shown in Fig. 6, the J_c curve of the $Sr_{0.6}K_{0.4}Fe_2As_2$ tapes in this work can be extrapolated to 20 T, where the J_c value is still above the practical level of 10^5 A/cm^2, indicating the tapes' great application potential in high-performance magnets for GHz nuclear magnetic resonance (NMR) and large accelerators [12].

The significant in-field performance of $Sr_{0.6}K_{0.4}Fe_2As_2$ tapes under different pressures is shown in Fig. 7, where the pinning force, $F_p = J_c(H) \times \mu_0 H$, is compared at $P = 0$ GPa and $P = 1.1$ GPa at 8 K and 12 K. The pressure of $P = 1.1$ GPa significantly improves the pinning force strength at 8 K from $F_p \sim 2$ GN m^{-3} to $F_p \sim 16$ GN m^{-3}, and from $F_p \sim 1.2$ GN m^{-3} to $F_p \sim 10$ GN m^{-3} at 12 K for field >6 T. This illustrates the significant improvement in superconducting performance of the $Sr_{0.6}K_{0.4}Fe_2As_2$ tapes.

IV. DISCUSSION

J_c is mostly limited by weak links (in the case of polycrystalline bulks), and thermally activated flux creep (an intrinsic property) emerges from weak pinning. High J_c values can, therefore, be achieved by a strong pinning force,

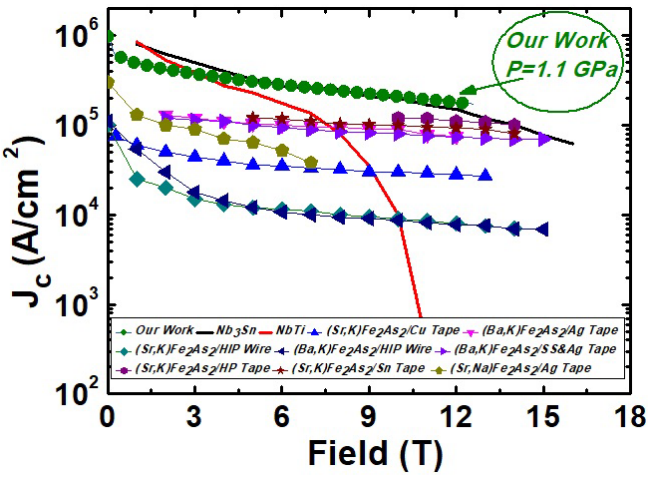

FIG. 6. Comparison of magnetic J_c values of our $Sr_{0.6}K_{0.4}Fe_2As_2$ tape with other best reported transport J_c values for different wires and tapes at 4.2 K [12,15,16,21–26]. In field >5 T, $J_c \sim 3 \times 10^5$ A/cm^2 was found in $Sr_{0.6}K_{0.4}Fe_2As_2$ tape under pressure, which is superior to the performance of low-temperature superconductors and other pnictide wires/tapes. Note: Presently, it is not possible to measure transport J_c under the hydrostatic pressure as this facility is not available on any transport measurement system. Therefore, we compared our magnetic J_c data to the other reported transport J_c data.

supplemented by the creation of effective pinning centers. Notably, hydrostatic pressure can induce pinning centers, leading to enhancement of the pinning force. It is well known that the formation energy of point defects decreases with increasing pressure [19,20,27]. The pinning force and the pinning centers are interrelated by $F_p = N_p f_p$ (here N_p is the number density of pinning centers, and f_p is the elementary pinning force, which is defined as the highest pinning strength of a pinning center, based on the interaction of the flux line

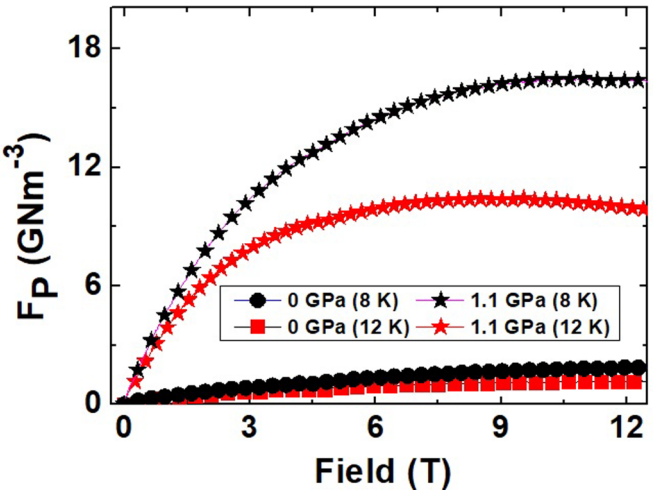

FIG. 7. Pinning force (F_P) as a function of field at $P = 0$ GPa and $P = 1.1$ GPa at 8 K and 12 K. At 8 K, $F_P \sim 16$ GN m^{-3} is obtained, increased from $F_P \sim 2$ GN m^{-3}. Similar enhancement can also be seen at 12 K.

with the defect). According to the flux pinning theory, strongly interacting defects can contribute to F_p individually, provided that $F_p \propto N_p$, while weakly interacting defects can contribute only collectively; the collective theory leads to $F_p \propto (N_p)^2$ for small defect numbers [28].

High pressure can modify grain boundaries, which can be approximated as potential wells, by reducing the width and height of the tunneling barrier. The critical current density J_c is then related to the width W and height H of grain boundaries as [Wentzel-Kramers-Brillouin (WKB) approximation] [29–31]

$$J_c = J_{c0} \exp(-2kW). \tag{3}$$

Here, $k = (2mH)^{1/2}/\hbar$ is known as the decay constant, m is the mass of the particle that is tunneling through the potential barrier, and J_{c0} is the critical current density at 0 T and 0 K. The derivative of $\ln J_c$ with respect to pressure can be written from Eq. (3) as [32]

$$\frac{d\ln J_c}{dP} = \frac{d\ln J_{c0}}{dP} - \left[\left(\frac{d\ln W}{dP}\right)\ln\left(\frac{J_{c0}}{J_c}\right)\right] - \frac{1}{2}\left[\left(\frac{d\ln H}{dP}\right)\ln\left(\frac{J_{c0}}{J_c}\right)\right] \tag{4}$$

$$= \frac{d\ln J_{c0}}{dP} + \kappa_{GB}\ln\left(\frac{J_{c0}}{J_c}\right) + \frac{1}{2}\kappa_H \ln\left(\frac{J_{c0}}{J_c}\right). \tag{5}$$

Here $\kappa_{GB} = -d\ln W/dP$ and $\kappa_H = -d\ln H/dP$ are the width and height compressibilities of the grain boundary, respectively. We assume, to a first-order approximation, that κ_{GB} and κ_H are nearly comparable to the average linear compressibility values $\kappa_a = -d\ln a/dP$ and $\kappa_c = -d\ln c/dP$ (here a and c are the in-plane and out-of-plane lattice parameters, respectively). From Eq. (5), we can therefore rewrite $d\ln J_c/dp$ as

$$\frac{d\ln J_c}{dP} \sim \frac{d\ln J_{c0}}{dP} + \kappa_a \ln\left(\frac{J_{c0}}{J_c}\right) + \frac{1}{2}\kappa_c \ln\left(\frac{J_{c0}}{J_c}\right). \tag{6}$$

To see the J_c dependence on pressure P, we take $\kappa_a \sim 0.013$ and $\kappa_c \sim 0.09$, as has been done in Ref. [33] for the similar material $SrFe_2As_2$. If $J_c \cong 2.12 \times 10^4$ A/cm^2 at 20 K and 0 GPa, then $[\kappa_a \ln(J_{c0}/J_c)] \approx 0.028$ and $[0.5\kappa_c \ln(J_{c0}/J_c)] \approx 0.096$. The second and third terms on right-hand side of Eq. (6) contribute nearly 6% to the experimental value, i.e., $d\ln J_c/dP = 2.23\,\text{GPa}^{-1}$ (Fig. 6). This indicates that the effects of hydrostatic pressure on geometric changes in grain boundaries, and hence, enhancement of J_c, are insignificant.

So, an obvious question arises: which phenomena are responsible for the enhancement of more than 90% in J_c? We argue here that this increase in J_c is the result of the increase in the number density of pinning centers. To support our argument, we analyzed pinning under pressure in $Sr_{0.6}K_{0.4}Fe_2As_2$ tape by using collective pinning theory. In collective pinning theory, $J_c(t)/J_c(o) \propto (1-t^2)^{5/2}(1+t^2)^{-1/2}$ in the case of δl pinning (spatial variation in the charge carrier mean free path l), whereas $J_c(t)/J_c(o) \propto (1-t^2)^{7/6}(1+t^2)^{5/6}$ relates to δT_c pinning (arising from randomly distributed spatial variation in T_c). Here, t is the reduced temperature and defined as $t = T/T_c$

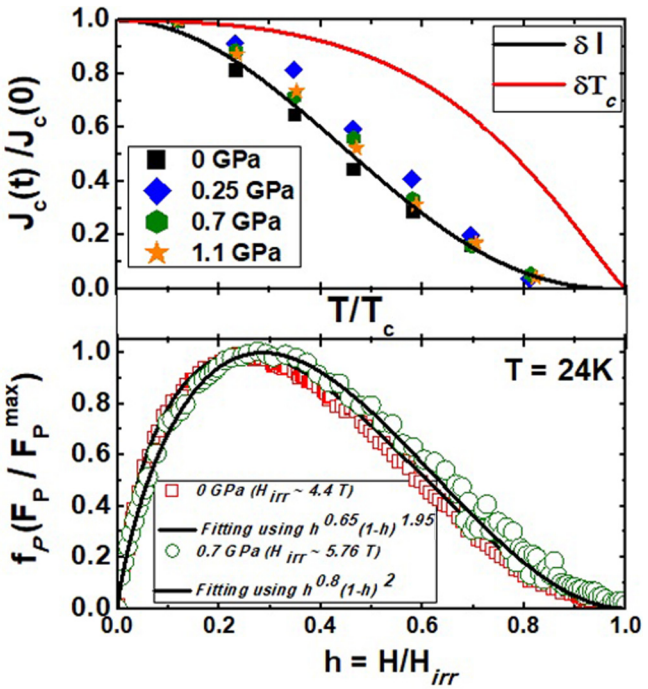

FIG. 8. Top panel shows $J_c/J_c(0)$ as a function of reduced temperature ($\tau = T/T_c$) at 0.05 T for $P = 0$,0.25,0.7, and 1.1 GPa. The experimental data points are in good agreement with theoretical δl pinning. The lower panel presents a plot of the vortex pinning force, normalized with respect to the maximum pinning force, versus reduced field (with respect to the irreversibility field, H_{irr}) at $P = 0$ GPa and $P = 0.7$ GPa, showing the transformation from normal core surface pinning to normal core point pinning.

[34]. The experimentally obtained J_c values and the expected theoretical variations for the δl and δT_c pinning mechanisms at 0.05 T are plotted together in order to examine the temperature dependence of J_c (top panel of Fig. 8). The $J_c(t)$ values can be found from the $J_c(B)$ curves at different temperatures. The experimental data found at $P = 0$,0.25,0.7, and 1.1 GPa correspond to the theoretical δl pinning. Therefore, δl pinning is dominant in $Sr_{0.6}K_{0.4}Fe_2As_2$ tape. The δl pinning is also found in MgB_2 under hydrostatic pressure [35]. Here, it is important to mention that the factor of flux creep is not taken into account and further work needs to be done to investigate the impact of flux creep on our analysis. To further probe the nature of the pinning mechanism, we plotted the pinning force $F_P = J_c \times B$ as a function of the reduced field $h = H/H_{irr}$, where H_{irr} is the irreversibility field, at different pressures and the fixed temperature of 24 K in the lower panel of Fig. 8. The H_{irr} is estimated by using the criterion of $J_c \sim 200$ A/cm^2. We used the Dew-Hughes formula, i.e., $F_p \propto h^m(1-h^n)$, to analyze the experimental data values; here, m and n are the scaling parameters used to determine the pinning mechanism [36]. We calculated $m = 0.65$ and $n = 1.95$ at 0 GPa, and $m = 0.8$ and $n = 2$ at 0.7 GPa. The Dew-Hughes model revealed that parameters $m \sim 1$ and $n \sim 2$ indicate normal core point pinning, and $m \sim 0.5$ and $n \sim 2$ indicate surface/grain boundary pinning in the case of δl pinning. Therefore, pressure transforms normal core surface pinning to normal core point pinning and hence induces more point pinning centers. The

insignificance of surface pinning at high pressures is due to the migration of low-angle grain boundaries in polycrystalline bulk samples, resulting in the evolution of giant grains, sacrificing surface pinning thereafter. Hence, a higher ratio of point pinning centers to surface pinning centers is expected under pressure.

Another piece of supporting evidence for the increase in the pinning center number density (N_p) under pressure is an estimation of the number of point pinning centers, which can suppress thermally activated flux creep, leading to J_c enhancement [37]. N_p is defined as

$$\frac{\Sigma F_p}{\eta f_p^{\max}} = N_P. \tag{7}$$

ΣF_p is the accumulated pinning force density, $f_p^{\max}$ is known as the maximum elementary pinning force (f_p), which is the interaction between a flux line and a single defect, and η is an efficiency factor. $\eta = 1$ corresponds to a plastic lattice, and the η value is otherwise $f_p^{\max}/B$ (where B is the bulk modulus of the material). We used the second order of approximation, so that the interaction between a flux line and a single defect is nearly same under pressure. Therefore, N_p is mostly dependent on ΣF_p and found to be increased, as enhanced pinning force was obtained at high pressure.

Most ideally, the direct experimental observations on the point defect and its density are through *in situ* HRTEM (high-resolution transmission electron microscopy) experiments. However, this is not possible as the hydrostatic pressure option is not available on any state-of-the-art HRTEM facilities.

V. CONCLUSION

In summary, we found that the high pressure of 1.1 GPa can significantly enhance J_c in $Sr_{0.6}K_{0.4}Fe_2As_2$ tape by one order of magnitude in both high and low fields. Remarkably, the obtained J_c values ($\sim 2 \times 10^5$ A/cm^2 at 4.2 K and 13 T) are the record highest compared with other pnictide wires/tapes and also, more significantly, with Nb_3Sn. The pressure-induced pinning centers are the prime sources of J_c enhancement, along with a fractional contribution from geometric changes around grain boundaries under pressure. We have demonstrated that hydrostatic pressure provides us with a route to significantly enhancing J_c beyond the cutoff (maximum) values observed in numerous superconductors that were produced using other existing approaches for J_c enhancement.

ACKNOWLEDGMENTS

X.L.W. acknowledges support from the Australian Research Council (ARC) through an ARC Discovery Project (No. DP130102956) and an ARC Professorial Future Fellowship Project (No. FT130100778). The work in China was supported by the National Natural Science Foundation of China (No. 51320105015), the Beijing Municipal Science and Technology Commission (No. Z171100002017006), and the Bureau of Frontier Sciences and Education, Chinese Academy of Sciences (QYZDJ-SSW-JSC026). Dr. T. Silver's critical reading of this paper is greatly appreciated.

[1] X. L. Wang, S. R. Ghorbani, Sung-Ik Lee, S. X. Dou, C. T. Lin, T. H. Johansen, K.-H. Müller, Z. X. Cheng, G. Peleckis, M. Shabazi, A. J. Qviller, V. V. Yurchenko, G. L. Sun, and D. L. Sun. Phys. Rev. B. **82**, 024525 (2010).

[2] X. L. Wang, S. R. Ghorbani, G. Peleckis, and S. X. Dou, Adv. Mater. **21**, 236 (2009).

[3] M. Miura, B. Maiorov, T. Kato, T. Shimode, K. Wada, S. Adachi, and K. Tanabe, Nat. Commun. **4**, 2499 (2013).

[4] H. Hosono and K. Kuroki, Phys. C (Amsterdam, Neth.) **514**, 399 (2015).

[5] W. Si, S. J. Han, X. Shi, S. N. Ehrlich, J. Jaroszynski, A. Goyal, and Q. Li, Nat. Commun. **4**, 1347 (2013).

[6] U. Welp, R. Xie, A. E. Koshelev, W. K. Kwok, P. Cheng, L. Fang, and H. H. Wen, Phys. Rev. B **78**, 140510 (2008).

[7] L. Fang, Y. Jia, C. Chaparro, G. Sheet, H. Claus, M. A. Kirk, A. E. Koshelev, U. Welp, G. W. Crabtree, W. K. Kwok, S. Zhu, H. F. Hu, J. M. Zuo, H.-H. Wen, and B. Shen, App. Phys. Lett. **101**, 012601 (2012).

[8] S. Graser, P. J. Hirschfeld, T. Kopp, R. Gutser, B. M. Andersen, and J. Mannhart, Nat. Phys. **6**, 609 (2010).

[9] D. Larbalestier, A. Gurevich, D. M. Feldmann, and A. Polyanskii, Nature (London) **414**, 368 (2001).

[10] M. G. T. Mentink, An experimental and computational study of strain sensitivity in superconducting Nb_3Sn, Ph.D. thesis, University of Twente, 2014.

[11] Y. Ma, Supercond. Sci. Technol. **25**, 113001 (2012).

[12] H. Hosono, K. Tanabe, E. T-Muromachi, H. Kageyama, S. Yamanaka, H. Kumakura, M. Nohara, H. Hiramatsu, and S. Fujitsu, Sci. Technol. Adv. Mater. **16**, 033503 (2015).

[13] P. Ilaria, E. Michael, M. Andrea, and P. Marina, Supercond. Sci. Technol. **28**, 114005 (2015).

[14] L. Wang, Y. Qi, D. Wang, X. Zhang, Z. Gao, Z. Zhang, Y. Ma, S. Awaji, G. Nishijima, and K. Watanabe, Phys. C (Amersterdam, Neth.) **470**, 183 (2010).

[15] G. Zhaoshun, T. Kazumasa, M. Akiyoshi, and K. Hiroaki, Supercond. Sci. Technol. **28**, 012001 (2015).

[16] H. Lin, C. Yao, X. Zhang, C. Dong, H. Zhang, D. Wang, Q. Zhang, Y. Ma, S. Awaji, K. Watanabe, H. Tian, and J. Li, Sci. Rep. **4**, 6944 (2014).

[17] T. Schneider and D. Di Castro, Phys. Rev. B **72**, 054501 (2005).

[18] C. P. Bean, Rev. Mod. Phys. **36**, 31 (1964).

[19] B. Shabbir, X. Wang, S. R. Ghorbani, C. Shekhar, S. Dou, and O. N. Srivastava, Sci. Rep. **5**, 8213 (2015).

[20] B. Shabbir, X. Wang, S. R. Ghorbani, A. F. Wang, S. Dou, and X. H. Chen, Sci. Rep. **5**, 10606 (2015).

[21] H. Lin, C. Yao, H. Zhang, X. Zhang, Q. Zhang, C. Dong, D. Wang, and Y. Ma, Sci. Rep. **5**, 11506 (2015).

[22] Z. Gao, K. Togano, A. Matsumoto, and H. Kumakura, Sci. Rep. **4**, 4065 (2014).

[23] P. Sunseng, T. Yuji, I. Hiroshi, K. Hideki, K. Norikiyo, A. Satoshi, W. Kazuo, and T. Tsuyoshi, Supercond. Sci. Technol. **27**, 095002 (2014).

[24] J. D. Weiss, C. Tarantini, J. Jiang, F. Kametani, A. A. Polyanskii, D. C. Larbalestier, and E. E. Hellstrom, Nat. Mater. **11**, 682 (2012).
[25] X. Zhang, C. Yao, H. Lin, Y. Cai, Z. Chen, J. Li, C. Dong, Q. Zhang, D. Wang, Y. Ma, H. Oguro, S. Awaji, and K. Watanabe, Appl. Phys. Lett. **104**, 202601 (2014).
[26] A. Iyo, N. Shinohara, K. Tokiwa, S. Ishida, Y. Tsuchiya, A. Ishii, T. Asou, T. Nishio, K. Matsuzaki, N. Takeshita, H. Eisaki, and Y. Yoshida, Supercond. Sci. Technol. **28**, 105007 (2015).
[27] A. Misiuk, Solid State Phenom. **19-20**, 387 (1991).
[28] H. R. Kerchner, D. K. Christen, C. E. Klabunde, S. T. Sekula, and R. R. Coltman, Phys. Rev. B **27**, 5467 (1983).
[29] J. Halbritter, Phys. Rev. B **46**, 14861 (1992).
[30] T. Tomita, J. S. Schilling, L. Chen, B. W. Veal, and H. Claus, Phys. Rev. B **74**, 064517 (2006).
[31] N. D. Browning, J. P. Buban, P. D. Nellist, D. P. Norton, M. F. Chisholm, and S. J. Pennycook, Phys. C (Amsterdam, Neth.) **294**, 183 (1998).
[32] T. Tomita, J. S. Schilling, L. Chen, B. W. Veal, and H. Claus, Phys. Rev. Lett. **96**, 077001 (2006).
[33] M. Kumar, M. Nicklas, A. Jesche, N. Caroca-Canales, M. Schmitt, M. Hanfland, D. Kasinathan, U. Schwarz, H. Rosner, and C. Geibel, Phys. Rev. B **78**, 184516 (2008).
[34] R. Griessen, W. Hai-hu. Wen, A. J. J. van Dalen, B. Dam, J. Rector, H. G. Schnack, S. Libbrecht, E. Osquiguil, and Y. Bruynseraede, Phys. Rev. Lett. **72**, 1910 (1994).
[35] B. Shabbir, X. L Wang, S. R. Ghorbani, S. X. Dou, and F. Xiang, Supercond. Sci. Technol. **28**, 055001 (2015).
[36] D. Dew-Hughes, Philos. Mag. **30**, 293 (1974).
[37] B. Shabbir, X. L. Wang, Y. Ma, S. X. Dou, S. S. Yan, and L. M. Mei, Sci. Rep. **6**, 23044 (2016).